

# Deliverable D33 (D4.12)

## Summary of AQ hotspot pilots, sustainability and associated benefits



### RI-URBANS

Research Infrastructures Services Reinforcing Air  
Quality Monitoring Capacities in European Urban &  
Industrial Areas (GA n. 101036245)

By



UNIVERSITY OF HELSINKI

04/04/2025

### Deliverable D33 (D4.12): Summary of AQ hotspot pilots, sustainability and associated benefits

Authors: Arnoud Apituley (KNMI), Diego Alves Gouveia (KNMI), Mirjam den Hoed (KNMI), Juliane L. Fry (Wageningen University), Pascale Ooms (Wageningen University), Bart Speet (TNO), Tim Vlemmix (KNMI), Benjamin Leune, Stephan de Roode (TU Delft), Gerard Hoek (UU), Jules Kerckhoffs (UU), Doina Nicolae (INOE), Jeni Vasilescu (INOE), Livio Belgante (INOE), Nora Zannoni (CNR), Angela Marinoni (CNR), Myriam Agró (UHEL), Cecilia Magnani (CNR), Valeria Mardonez (CNR), Laura Renzi (CNR), Ferdinando Pasqualini (CNR) & Camilla Perfetti (CNR).

<b>Work package (WP)</b>	WP4 Pilot implementations for testing and demonstrating services
<b>Deliverable</b>	D33 (D4.12)
<b>Lead beneficiary</b>	UU
<b>Deliverable type</b>	<input checked="" type="checkbox"/> R (document, report) <input type="checkbox"/> DEC (websites, patent filings, videos,....) <input type="checkbox"/> Other: ORDP (open research data pilot)
<b>Dissemination level</b>	<input checked="" type="checkbox"/> PU (public) <input type="checkbox"/> CO (confidential, only members of consortium and European Commission)
<b>Estimated delivery deadline</b>	M43 (30/04/2025)
<b>Actual delivery deadline</b>	04/04/2025
<b>Version</b>	Final
<b>Reviewed by</b>	WP4 leaders and project coordinators
<b>Accepted by</b>	RI-URBANS Project Coordination Team
<b>Comments</b>	This report summarizes experiences in RI-urbans pilot studies with complementary approaches to traditional AQMS in order to characterize air pollution hotspots. We finish with a reflection on upscaling and sustainability.

## Table of Contents

<b>1. ABOUT THIS DOCUMENT</b>	<b>1</b>
<b>2. AIMS OF THE DELIVERABLE</b>	<b>1</b>
<b>3. ROTTERDAM PILOT USING REMOTE SENSING</b>	<b>2</b>
3.1 MEASUREMENT STRATEGY	2
3.1.1 Vertical Profiling	2
3.1.2 Airborne mapping	4
3.1.3 Mobile observations	4
3.2 VERTICAL PROFILING MEASUREMENT EXAMPLES	5
3.3 AIRBORNE MAPPING EXAMPLE	7
3.4 MOBILE OBSERVATIONS EXAMPLES	8
3.4.1 Car based observations	8
3.4.2 Bicycle observations	9
<b>4. ROTTERDAM CAR-BASED MOBILE MONITORING</b>	<b>10</b>
4.1 MONITORING STRATEGY	10
4.2 RESULTS	12
<b>5. BUCHAREST PILOT</b>	<b>13</b>
5.1 MEASUREMENTS STRATEGY	13
5.2 FIXED MEASUREMENTS	13
5.3 MOBILE MEASUREMENTS	15
<b>6. MILAN PILOT</b>	<b>16</b>
6.1 MEASUREMENT STRATEGY	16
6.2 BACKGROUND URBAN REFERENCE SITE	16
6.3 MILANO LINATE HOT-SPOT SITE	21
6.4 URBAN MAPPING WITH MOBILE MEASUREMENTS	23
6.5 COMPARISON BETWEEN HOT SPOT-SITES AND REFERENCE SITE	24
<b>7. POTENTIAL FOR SUSTAINABILITY AND UPSCALING IN CITIES</b>	<b>25</b>
<b>8. REFERENCES</b>	<b>27</b>

## 1. ABOUT THIS DOCUMENT

This document summarises results from the task on quantifying emission sources and concentrations in and near urban areas with intense traffic and/or industrial activities, and to identify the contribution of these hot spots to air pollutant exposure. With WP1 data, this task will assess the regional background with novel observations within and near the hot spot areas. The data will be linked through regional and high-resolution modelling (WP3). Initial results from the pollution hotspots are depicted in D4.11. In Rotterdam, mobile monitoring will be done using a car measuring nanoparticles, BC, NO<sub>2</sub>, PM<sub>2.5</sub> and CO<sub>2</sub>, in addition to a network of stationary citizen NO<sub>2</sub> and PM<sub>2.5</sub> sensor measurements.

The new Ambient Air Quality Directive (EU) 2024/2881 is requiring that the highest pollution hotspots should be identified and air quality measurements carried out there, with a ratio urban background/hotspot ratio not higher than 2. The methods used here are valid for this identification, not only for new pollutants but also for criteria pollutants. In this sense the mapping of pollutants at urban scale is a very powerful tool for implementing this new directive.

Remote sensing techniques will be applied and will provide an important input. Models and observations will be compared to demonstrate the ability for upscaling in other cities. In Milan, an urban pollution map will be created with special attention to heavy traffic roads, while in Bologna focus will be on the airport (<4 km away). Mapping will be carried out with mobile sensors for gases, PM and BC. A comparison of measurements with urban scale LUR and DALES models and microscale chemical transport models will be made. Bucharest set up an observation site in a highly polluted area around one of the most important power plants in the city. In-situ and remote sensing observations near the pollution source and at the background reference site are used to quantify nanoparticles, as well as mobile measurements.

This document is delivered to the European Commission as RI-URBANS deliverable D33 (D4.12) and shared with all RI-URBANS partners for their use. It will also be made available in the public domain, <https://riurbans.eu/work-package-4/#deliverables-wp4>.

## 2. AIMS OF THE DELIVERABLE

The aim of this Deliverable D33 (D4.12) is to present:

- Summary of the pilot studies, including methods, results (maps, plus numbers) and required resources.
- Potential for upscaling and sustainability for cities

We first discuss results per pilot (Rotterdam, Milan, Bologna, Bucharest) and then present an overall assessment.

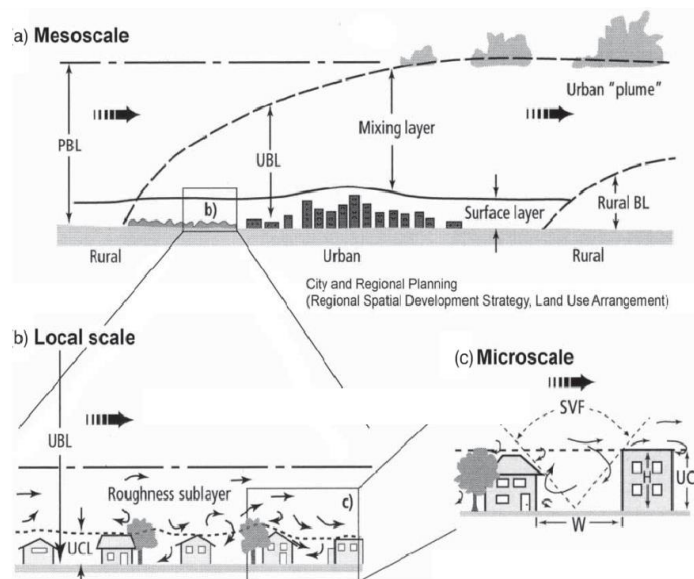
### 3. ROTTERDAM PILOT USING REMOTE SENSING

#### 3.1 Measurement strategy

##### 3.1.1 Vertical Profiling

Rotterdam was selected as one of the pilot cities for hot-spots. One of the main design aspects of the pilot study was to include vertical profiling observations of aerosol profiles (as a proxy of air pollution) and wind (in order to better grasp the dynamics). Figure 3.1. Explains the rationale in schematic form. The vertical build-up of the atmosphere in and around an urban area is shown here. The influence of the urban canopy, going from the micro scale (c) up to the mesoscale (a) is to be taken into account assessing the (health) effects of hot spots. The mixed layer height is an important parameter since it defines to a large extent the volume in which the pollution from a hot spot can be mixed and diluted. Therefore, estimations of the MLH as well as the wind in the area associated with the pollution hot spot (source) and the surrounding areas is important to understand the distribution of air pollution. Therefore, ceilometers, measuring vertical distributions of aerosols as a proxy for air pollution as well as vertical wind profiles, to measure the driving force for dispersion, were measured in the city. These observations were used for testing the implementation of urban canopies in the LES model DALES.

This measurement strategy was deployed during the hot-spot pilot study in Rotterdam that was conducted in September 2022. The Dutch atmospheric research community called Ruisdael Observatory collaborated in this study.



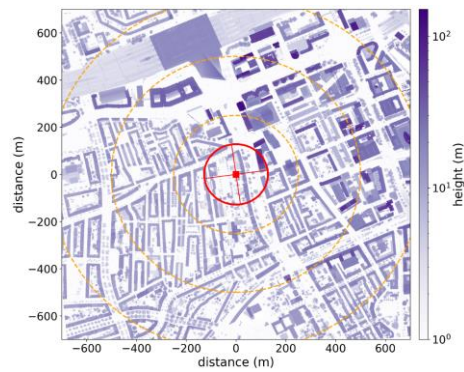
**Figure 3.1.** Schematic illustration of the vertical build-up of the atmosphere at scales from city to street level, indicating atmospheric layering and atmospheric dynamical processes that play a role in the dispersion of air pollution.

Figure 3.2 shows the domain of the Rotterdam area that includes air pollution hot spots due to road traffic, transport over water and industrial activity in the harbour (power plants, petrochemical industry, manufacturing). In addition, a regional airport is situated close to the residential area. In the map, the locations of vertical profiling instruments are indicated. Since the prevailing wind is from West to East, relatively clean air is advected from over the North Sea, taking up the air pollution over the harbour and industry, towards the residential area, and subsequently further inland. By strategically placing the vertical profiling instruments along this trajectory, the development and dynamics of the hot spot emissions can be observed. The observations can be used to verify and possibly improve computational models applied to the urban area in full complexity. The implementation of the (Rotterdam) urban canopy were made in the LES model DALES.

In all four locations indicated in Fig.3.2 ceilometers were installed that monitored the vertical distribution of aerosols in the planetary boundary layer, including an instrument right in the city centre (see Figure 3.3). Vertical profiles of wind were measured also in the city centre, as well as in the Cabauw station. Furthermore, the Cabauw station (ACTRIS National facility) served as a location with detailed information of atmospheric state and composition at ground level as well as in the vertical dimension.



**Figure 3.2.** Location of lidar instruments for vertical profiling during the Rotterdam campaign in September 2022.



**Figure 3.3.** Illustration of the location of the ceilometer and wind profiler in the city centre of Rotterdam. High rise buildings are blocks away.

### 3.1.2 Airborne mapping

Since satellite observations of air pollution have become more accurate and have become available at higher spatial resolutions, such as the Sentinel-5p/TROPOMI instrument that provides daily maps of NO<sub>2</sub> tropospheric columns around solar noon at a resolution of about 3.5x3.5 km resolution. This resolution is high enough to distinguish areas of higher and lower concentrations in a city like Rotterdam. However, in order to see hot spots and to study the dispersion of air pollution, even higher resolutions are needed and also more frequent observations, rather than once per day. The use of an experimental airborne mapping instrument (Spectrolite) was deployed on several test flights over the Rotterdam area shown in Fig. 3.2. Spectrolite is aimed to deliver pollution maps at a resolution of tens of square meters. These results can be used to fill the gap between the TROPOMI observations and the resolutions that are needed for the hot spot studies.

### 3.1.3 Mobile observations

Urban street trees can affect air pollutant concentrations by reducing ventilation rates in polluted streetcanyons (increasing concentrations), or by providing surface area for deposition (decreasing concentrations). Similar to the measurement strategy deployed in the Task 4.3 of urban scale mapping (see chapter 4), an instrumented car was deployed in the September 2022 Rotterdam campaign, using mobile measurements of nitrogen dioxide (NO<sub>2</sub>), particulate matter (PM), black carbon (BC), and ultrafine particles (UFP).

In the framework of the RITA-2022 urban air quality measurement campaign coupled to RI-URBANS, an innovative approach was implemented to measure nitrogen dioxide (NO<sub>2</sub>) and black carbon (BC) in the Rotterdam region. The campaign aimed to create a high-resolution map of urban air pollutants, a key part of monitoring the effects of the energy transition on air quality. Mobile measurements were carried out along a fixed 20 km cycling route from the Rijnmond Environmental Service (DCMR) building in Schiedam to the centre of Rotterdam and back, with citizen volunteers playing a crucial role. This fixed circuit not only provided detailed snapshots of air quality variations related to traffic density and urban structure, but also helped to ensure repeatable and insightful data. This methodology may have strengthened the relationship between scientific research and social engagement, and the acquired data set, pending verification, has the potential to validate the urban air quality system (RETINA, Mijling, 2020) for the Rotterdam region in the future.

### 3.2 Vertical profiling measurement examples

Figures 3.4 to 3.6 show examples of the vertical profiling measurements with the wind lidar and ceilometers. An example for 1 September 2022 of the horizontal wind speed profile in the city centre of Rotterdam is shown in Figure 3.4. During daytime roughly between 7 AM and 7 PM (UTC) the wind profile shows much more similarity between 40 m and 240 m above ground level than during the night. This is a consequence of the growth of the boundary layer during the day due to rising warm air.

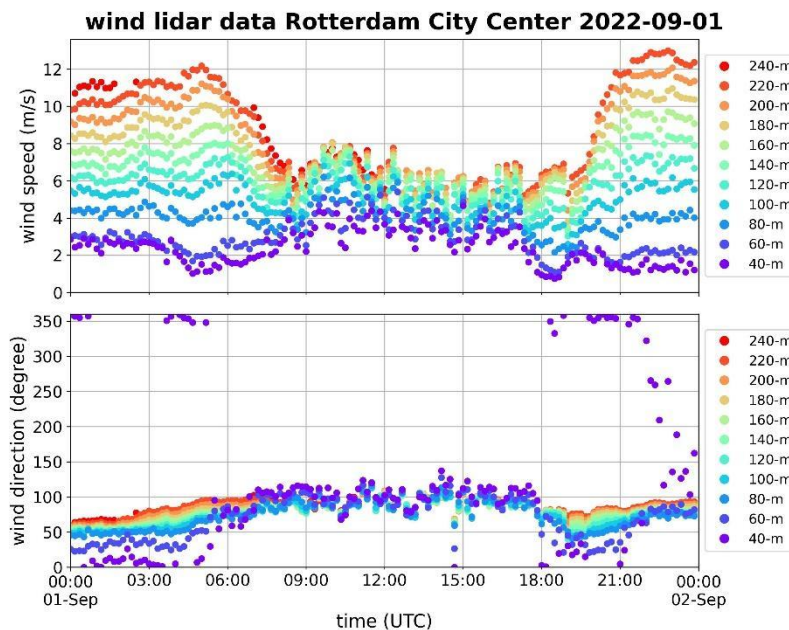


**Figure 3.4.** Example of wind profile observations in the centre of Rotterdam for a single day, 1 September 2022.

For the same day as in Figure 3.4 (1 September 2022), Figure 3.5 shows the vertical distribution of aerosols during the day at the measurement locations from West to East over the campaign area, including the Cabauw station to the East of Rotterdam. In the aerosol profiles the growth of the boundary layer can be seen from 7 AM (UTC) until mid-day. At the end of the day 7 PM (UTC) the rising motion of air stops, but the aerosols and pollution remain in a well-mixed layer up to about 2 km altitude.

Although the overall behaviour of the boundary layer is similar between the four locations (the maximum boundary layer depth reached is about 2 km for all stations as well as the time during the day when that happens), close inspection of the dynamics of the boundary layer height shows differences in behaviour between the stations. This is due to the local conditions of surface temperature and surface roughness. The development of the mixed layer height can often be followed by the somewhat trained human eye. However, getting automated numerical

estimates for MLH is a challenging task. The ceilometer profiles are submitted to the E-Profile ALC network and MLH values are derived using the STRATFINDER algorithm (Kotthaus et.al, 2023).

The combination of the wind profiles, in the city (shown in Figure.3.4) and outside of the city (not shown here) together with the vertical distribution of aerosols as a proxy for air pollution provide essential information to analyse the dispersion of air pollution away from the hot-spots.

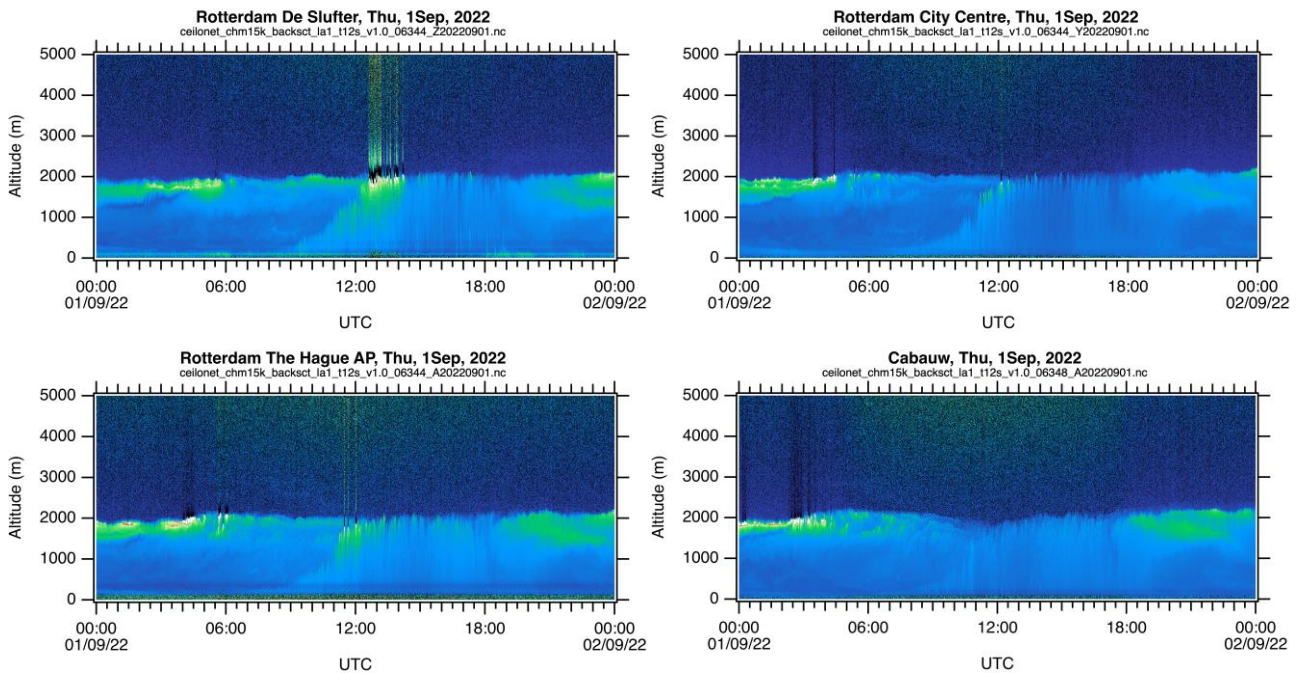


**Figure 3.5.** Example of ceilometer observations for a single day, 1 September 2022, at four locations in and around Rotterdam. From West ‘De Slufter’ to East ‘Cabauw’. Refer to the map in Figure 3.2 for the locations. The ceilometer in the city center is co-located with the Doppler wind lidar shown in Figure 3.4. The colours are relative units representative of the aerosol backscatter. Darker blue is aerosol poor air, lighter colours have more aerosol scattering. White represents clouds or very strong backscatter.

High resolution modelling was applied to the city including the urban canopy. An example of a validation activity of the use of the vertical wind profile observations in the city of Rotterdam against the LES modelling is shown in Fig.3.6. In the example it is shown that the implementation of the urban canopy has improved the modelling result for the vertical wind profile.

## Validation with wind lidar

- Surface layer too shallow
- Individual buildings not resolved by LES!
- Add bulk canopy drag:
  - $\partial u_i / \partial t = -\rho_b c_d |U| u_i$
  - $\rho_b$  = building area density =  $f(x,y,x)$  derived from AHN height map (experimental!)
  - Improvement, but further tuning/testing required...

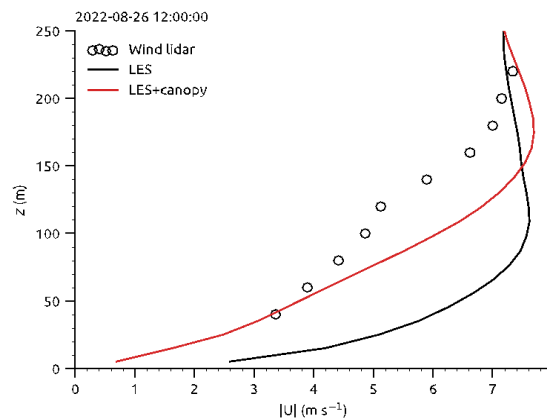


**Figure 3.6.** An example of a comparison between LES modelling of the vertical wind profile over de city of Rotterdam compared to the wind profile from Doppler wind lidar on 26 August 2022.

### 3.3 Airborne mapping example

In Fig. 3.7 an example is shown for the flight from Spectrolite on 1 September 2022. This was a day without low clouds which can be seen from the ceilometer observations on that day, presented in Figure 3.5. The ceilometer collected at four locations in the Rotterdam area also show that the area mapped by the flight was indeed cloud free. Since the remote sensing instrument was looking downward from the aircraft, all the NO<sub>2</sub> observed from the plane was in the mixed layer. However, due to the limitations on the flight level that was allowed by air traffic control (below 2 km), a small fraction of the polluted boundary layer was not captured in the vertical column density (VCD). The VCD can be regarded as a measure for the average NO<sub>2</sub> concentration in the total thickness of the atmosphere below the aircraft. In the VCD map, a clear distinction can be seen between the higher values (red) and the lower values (blue). It should be noted that the image shown is a preliminary result and that certain effects, in particular due to the brightness differences of the surface still have to be improved.

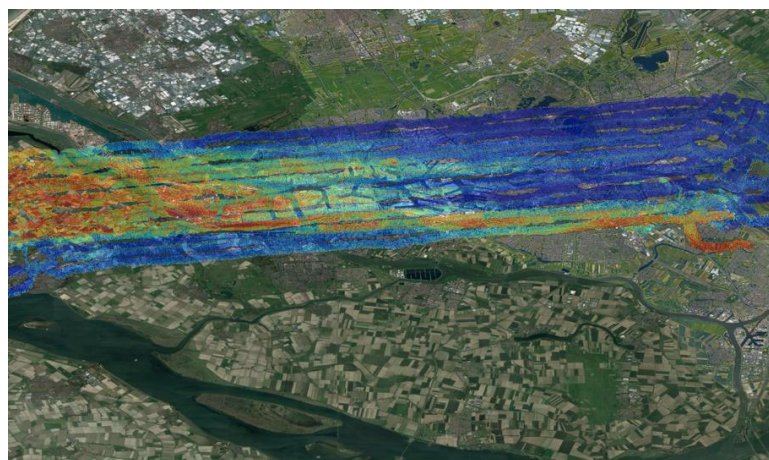


**Figure 3.7.** The NO<sub>2</sub> vertical column densities from the Spectrolite instrument for the flight over Rotterdam on the afternoon of 1 September 2022. The colour scale is in relative arbitrary units. Blue colours indicate a lower NO<sub>2</sub> vertical column density, the red shades represent higher values.

### 3.4 Mobile observations examples

#### 3.4.1 Car based observations

During the measurement campaign, we deployed an instrumented car from Utrecht University equipped with a fast (50 litres per minute) inlet manifold and multiple pollutant monitors. The car was equipped with fast-response instrumentation to measure NO<sub>2</sub> (Aerodyne Research, Inc. CAPS monitor), BC (Magee Scientific AE33 aethalometer), UFP number count (TSI EPC 3783), and PM<sub>2.5</sub> (TSI DustTrak), all at 1 second time resolution. A Global Positioning System recorded the location. Measurements were conducted between 6 am and 6 pm local time on all days of the week, covering various parts of the city on different days. (Fry et al., 2025). Results are shown in Figure 3.8, while in Figure 3.9 an attribution is made according to the various locations throughout the city and related pollution sources. Note that the airport and harbour are indicated.

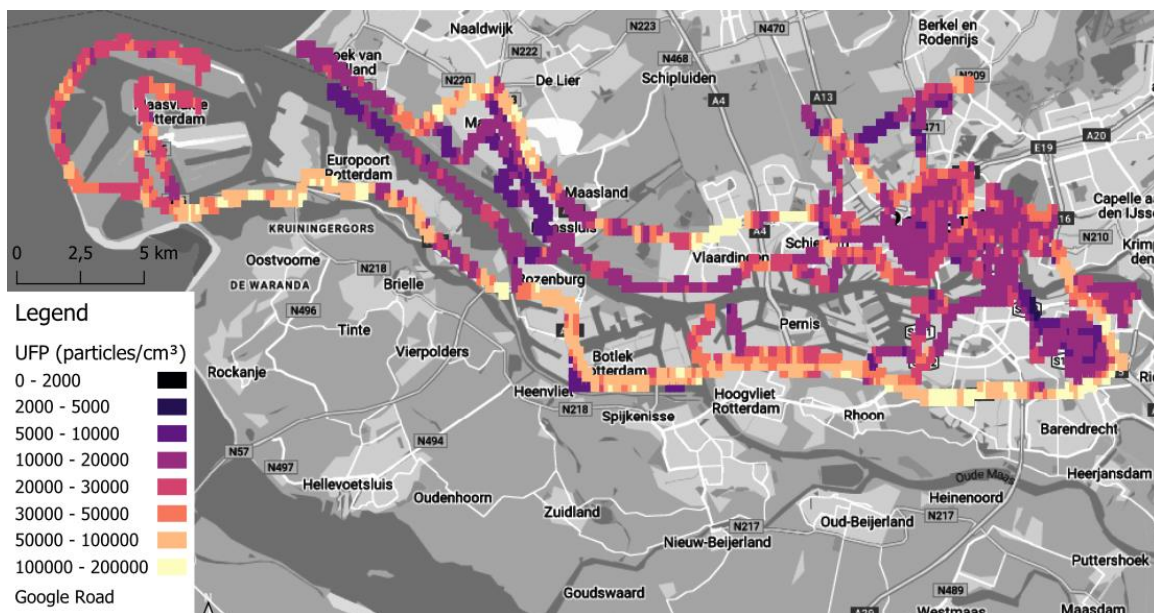


**Figure 3.8.** Average UFP concentrations averaged to a 200x200m grid. Spatial patterns show highest levels of UFP on highways (A15 & A20) and along a provincial road (N223).

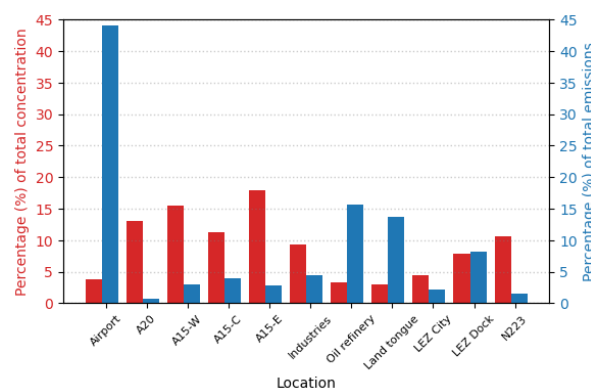


**Figure 3.9.** Percentage contribution to total concentrations (red) and emissions (blue).

The airport area shows larger share of predicted emissions than concentrations, but data was sparse, and thus potentially not representative flight activity. Highways show larger share in concentrations than emissions, suggesting that automotive and freight vehicle traffic may be a larger source of UFP than captured in emissions factors.

### 3.4.2 Bicycle observations

Instrumented bicycles (Figure 3.10) were driven on a prescribed track around the city by volunteers to obtain repetitive measurement of nitrogen dioxide (NO<sub>2</sub>) and black carbon (BC). The track was designed along a ~19 km loop from Schiedam towards the Rotterdam city center and back between 22 August - 8 September 2022. This was to generate high-resolution maps of NO<sub>2</sub> and BC of the Schiedam-Rotterdam area and identify air pollution hot-spots. The instruments deployed were a self-developed, accurate in-situ NO<sub>2</sub> sensor (Sluis et al., 2010) and a portable aethalometer (provided by VITO) mounted on a bicycle ridden by volunteers.

A group of 22 volunteers, including KNMI and DCMR staff, RITA-2022 participants, students, and engaged citizens, contributed by operating the measurement equipment while cycling. This broad involvement not only yielded an extensive data set, but also potentially strengthened the link between science and society. Figure 3.10 shows the instrumented bicycles and Figure 3.11 shows the results from the track on 29 August 2022 around noon as an example. The data show concentration variations that seem to be associated with traffic density and city infrastructure. This high-resolution dataset forms a valuable basis for further analysis and for comparisons with the stationary monitoring network, models, and other innovative datasets collected during the RITA-2022 campaign that can be related to RI-URBANS.



**Figure 3.10.** Instrumented bicycles were driven on a prescribed track around the city by volunteers.

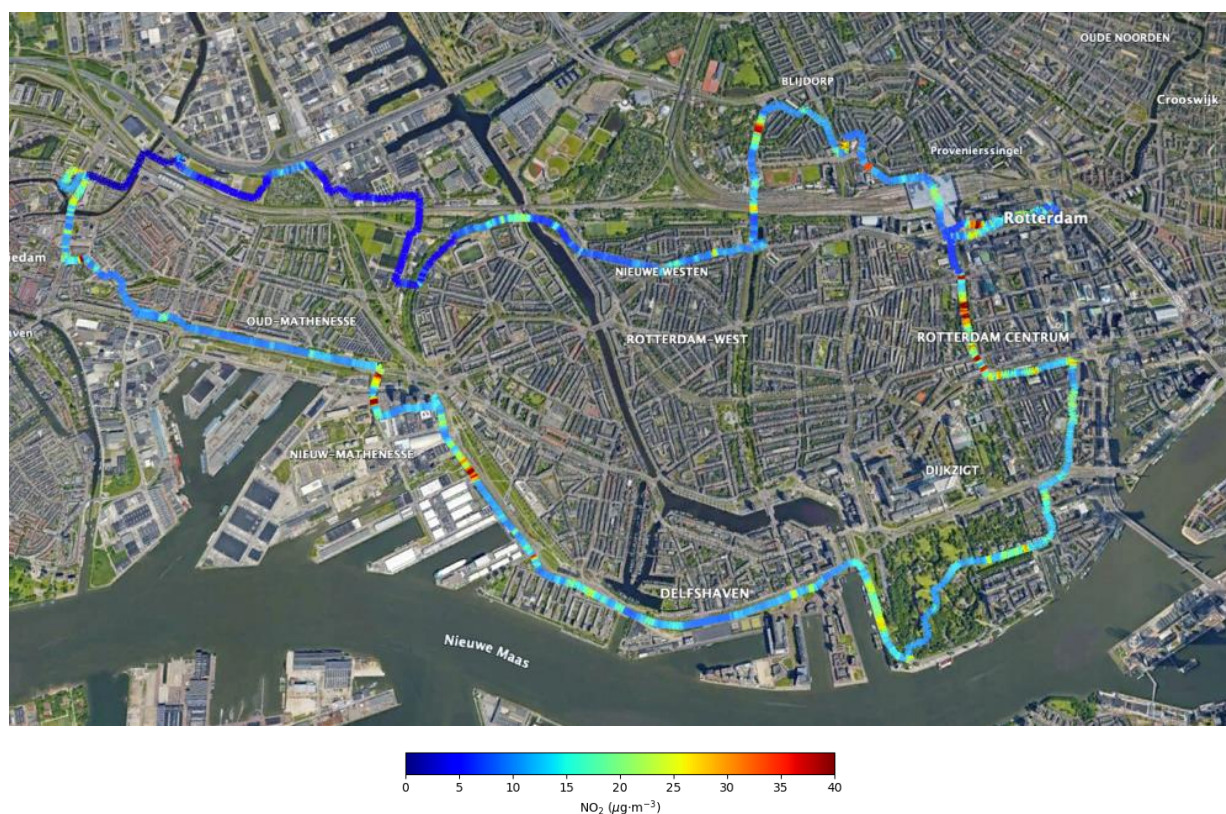


**Figure 3.11.** The result for 29 August 2022 between 11:00-13:00 CEST. Blue colors indicate low concentrations, while red indicates high concentrations.

The NO<sub>2</sub> data collected have not yet been fully validated. Mobile measurements are inherently challenging to use for model validation or data assimilation, primarily due to the discrepancy in temporal representativeness: While mobile measurements provide a snapshot that lasts only a few seconds, the model time resolution is approximately one hour. Fortunately, choosing to repeatedly cycle a fixed circuit (at different times of the day) provided significantly more insights than an alternative approach that would map a distinct part of the urban region under study for each iteration.

## 4. ROTTERDAM CAR-BASED MOBILE MONITORING

### 4.1 Monitoring strategy

the aim was to produce long-term average air pollution concentration maps for the area, by the means of Land Use Regression (LUR) models. A sub-question was to investigate if the industrial sources (mainly port activities) could be adequately captured in the mobile monitoring campaign.

We used a car to measure the ambient concentrations of NO<sub>2</sub>, BC and UFP during two seasons in the city of Rotterdam; one campaign in November-December 2022 and another campaign in May-July 2023. The car was equipped with lab-grade 1 Hz NO<sub>2</sub> (CAPS, Aerodyne Research Inc., USA), 1 Hz BC (AE33, Magee Scientific), and 1 Hz UFP (EPC 3783, TSI) monitors measuring simultaneously. A Global Positioning System (GPS) (G-Star IV, GlobalSat, Taiwan) was used to record the location of the car, which was linked to the measuring equipment via date and time.

The measurements were mainly carried out between 8 to 22 hours every day in the study period (including some weekend days) in different parts of the city. The study area extended beyond the municipality of Rotterdam to cover sources in the area more broadly, include the harbour, industrial area, and airport. The “route” was discussed in detail with DCMR, the regional authority for the environment.

The study design was mostly a dedicated approach, but had elements of an opportunistic approach. The dedicated part comes from the fact that the area was divided into 8 polygons, each containing a part of the city centre and residential areas as to randomize road characteristics at much as possible in each polygon. Drivers were instructed to drive in one polygon for each morning or afternoon session. Polygons were driven multiple times, each on a different day of the week and part of the day. The opportunistic part is that there were no specific routes that were followed. Drivers were asked to drive randomly on busy roads, residential roads and in industrial areas. Thus, the campaign does not rely on choices made by individuals for other reasons, such as the shortest route between home and work, as in the citizen-based campaign (Baxter, et al., 2013, Kerckhoffs, et al., 2016, 2017, Kumar, 2015, Shen, 2022).

This way, we made sure there is temporal dependencies in the data and no temporal correction is needed in the data processing. This is because all types of roads and corresponding co-variates were driven at different timepoints throughout the day and week, therefore, effectively nullifying the correlation between the covariates and time of day. The number of repetitions per location is quite low (or absent) complicating measured data interpretation. The number of repetitions was low by design because the main purpose was to develop a model for which repetitions are not essential. Though winter and summer campaigns were used some bias arises from the fact that the driving was mainly on weekdays between 09:00h and 19:00h CET or CEST.

The time resolution of all our instruments was 1Hz. Though only the UFP device was accurate enough on this time base that no post-processing was needed other than deleting unrealistic values below 500 particles/cm<sup>3</sup> and above 5000000 particles/cm<sup>3</sup>. For the BC and NO<sub>2</sub> device the 1-sec resolution gave too much noise, so a moving average of 6 sec and 3 sec was used, respectively.

All instruments used are lab-grade and not very portable by hand. At least, a car is needed to make use of these instruments in a true mobile setup. Colocation with reference measurements was done, but not checked thoroughly enough during monitoring campaign, leading to unreliable NO<sub>2</sub> measurements in the winter campaign.

On top of that, we also validated the UFP measurements by driving our measurements car right after another exactly the same measurement car (used in other projects). Results show that a moving platform can very accurately pick up UFP concentrations while driving (Figure 4.1). Despite this QA-QC, mobile measurements of NO<sub>2</sub> during the winter campaign were lower than during the summer campaign and substantially lower than measured at routine monitoring sites in Rotterdam. Additional QA-QC is needed.

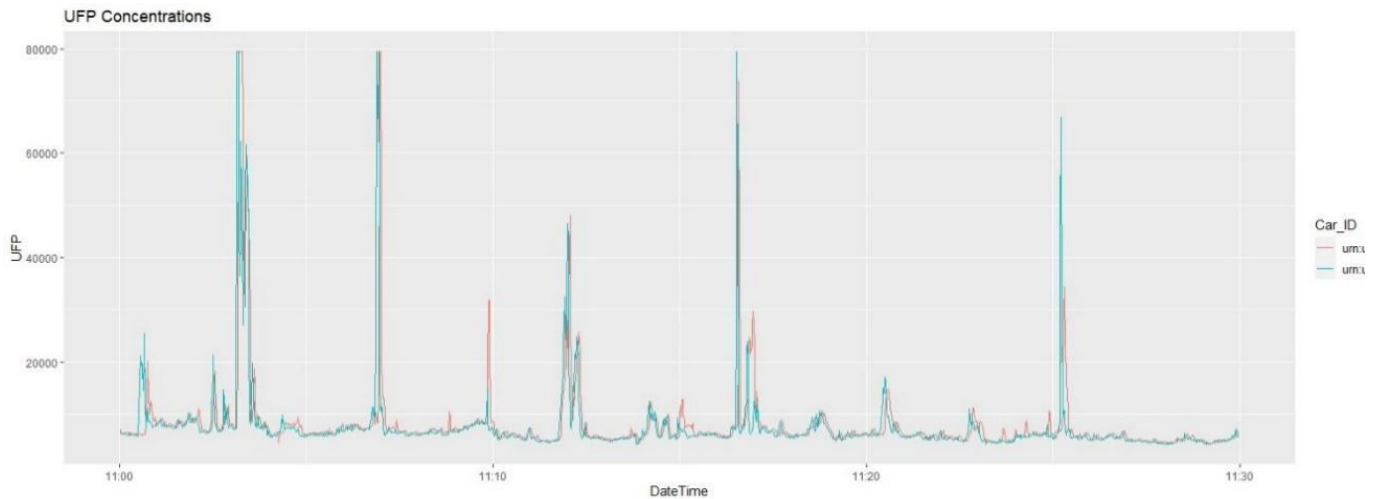


**Figure 4.1.** Example of UFP measurements (particles/cm<sup>3</sup>) by two cars.

## 4.2 Results

New Particle Formation (NPF) was probably seen on summer afternoon. As UFP data are scarce in the Netherlands this is an important confirmation of this phenomenon in a rather ‘northern town’ albeit with many UFP precursors (seagoing ships, refineries, in addition to traffic).

Mobile monitoring adds a lot of extra spatial variation in maps of air pollution, provided no high-resolution AQ modelling is available. For UFP, currently not modelled and hardly monitored, the campaign did generate a lot of new/additional data and seemed to confirm NPF. However, due to the scarcity of repetitions the data is hard to compare to existing modelled data (unlike the cycling data). This also limits the interpretation of the new UFP data in relation to the well-established monitored and modelled data on other pollutants (e.g. BC, NO<sub>x</sub>, PM).

We had hoped to compare UFP/BC or UFP/NO<sub>2</sub> ratio’s but due to data issues, few repetitions/ too few observations it is hard to draw conclusions. With systematic mobile monitoring in areas of interest, generating sufficient repetitions the mobile approach could have been more successful in mapping specific source areas. Ratios between pollutants offer new insights into the source contribution of the pollutants. E.g. UFP is often elevated near airports, whereas BC and NO<sub>2</sub> are not. Similarly, one might expect to see areas with the influence of seagoing ships (supposedly the largest UFP source in the area), and the refineries. Figure 4.2, does seem to suggest some of the expected influences in some parts, but produces unexpected results in others. The area near the airfield has similar colours as Barendrecht to the south of Rotterdam. From the map one could conclude either that there are two airports or that the info on the map is not indicative for an airport.

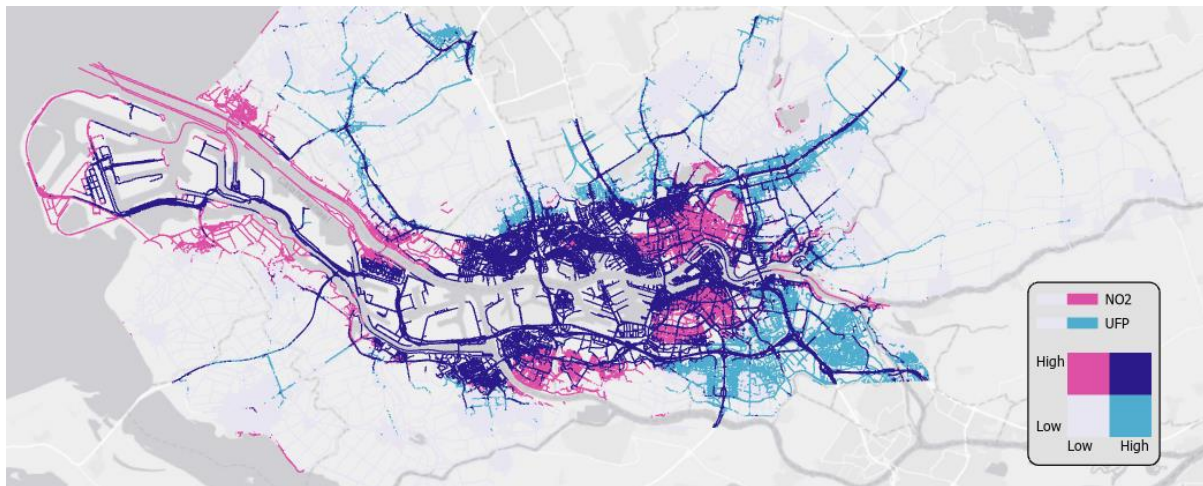


**Figure 4.2.** Ratio between predicted NO<sub>2</sub> and UFP concentrations in Rotterdam. Each of the four colours in the 2x2 box represent an equal number of road segments.

## 5. BUCHAREST PILOT

### 5.1 Measurements strategy

The Bucharest hotspot campaign aim was to evaluate particulate matter and NO<sub>x</sub> levels near a power plant during intense and low heat producing capacity periods. A detailed description of the pilot set-up and findings is available in D32 (D4.11). Two strategies for measurements have been conducted in Bucharest using fixed and mobile measurements to reveal the pollution levels nearby the selected hotspot, CET Vest power plant. This power plant started a modernization process in 2020, but it is still considered one of Bucharest's significant industrial polluters, ranking as the second-largest emitter of particulate matter and gasses among energy providers according to the reports of the National Environmental Agency.

Fixed measurements strategy involved to set up a temporary site, nearby the CET Vest power plant during May-November 2022. Concomitant measurements of the same atmospheric variables using in-situ and remote sensing instruments at the temporary site and the reference site, RADO-Bucharest ACTRIS national facility, have been performed. Main instruments used during this pilot studies at the reference site were: ceilometer, wind lidar, lidar system, optical particle counter EDM180 Grimm. While, at the temporary have been deployed: ceilometer, wind lidar, lidar, gas monitors, an optical particle counter.

Mobile measurements strategy had been conducted together with the urban mapping task in RI-URBANS, when mobile measurements of particle matter and NO<sub>2</sub> in a dense residential area close to the hotspot were performed during winter (2023) and summer (2022) periods. The car has been equipped with different sensors measuring simultaneously: a UFP sensor (Naneos Partector 2, 1 s), particle and gaseous sensors (Ecomesure EcomTrek - 10 s and/or Sniffer4D V2, 1 s) and a GPS (Navilock NL-442U, 1s) to independently save the geographic coordinates.

### 5.2 Fixed measurements

The aerosol near-surface data collected in the 2022 (May-August) with the two similar optical particle counters have been analysed from the perspective of air quality, to identify special events with increased mass concentrations of particulate matter fractions (PM<sub>1</sub>, PM<sub>2.5</sub> or PM<sub>10</sub>). The daily concentrations of particulate matter presented a similar variability at both sites, with overall higher values at the reference site (MARS) for PM<sub>10</sub>, while fine particle (PM<sub>1</sub>) dominated at the temporary site in Bucharest (INCAS) during the entire period.

The traffic-related peaks are visible in the diurnal cycle of the ratio  $PM_{2.5}$  to  $PM_{10}$  at the reference site. At the temporary site, close to the hotspot, there is no clear diurnal cycle, leading to the assumption that the hotspot is a constant source of smaller particles, overlaying to traffic-originated particles (Figure 5.1).

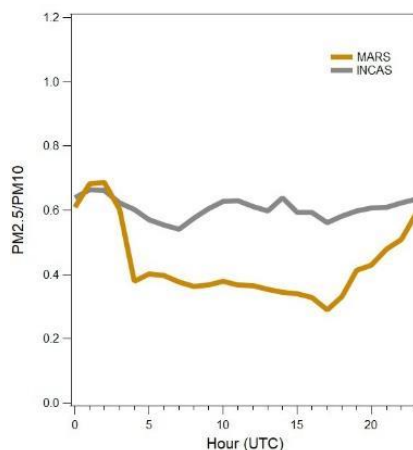


**Figure 5.1.** Diurnal pattern of the ratio  $PM_{2.5}$  to  $PM_{10}$  at MARS and INCAS: average hourly values over the entire campaign.

Comparative remote sensing data have been analysed as averaged values representative for warm and cold seasons, to assess the vertical distribution of aerosol particles and calculate the mixing layer height (MLH) (Figure 5.2). The median MLH at both locations during summer is approximative 2500 m, and during autumn approximative 1000 m. The seasonal diurnal cycles for MLH evaluation pin-pointed that the hourly average of MLH is higher at the temporary site location on both seasons during the entire day. It can be noticed difference on the maximum MLH, for example on cold season the maximum MLH for temporary site is reached around 14 UTC, while for reference site one hour later. This behaviour is favoured by the urban heat island in the city.

The only situation which would favour the transport of pollutants from the power plant to the residential area is during winter night time, when the planetary boundary layer is very low, the pollutants are injected above and transported by mid-tropospheric winds from the southern sector (SE-S-SW). The minimum MLH is reached during night time (23:00 – 05:00 UTC) and is below 400 m for both seasons.

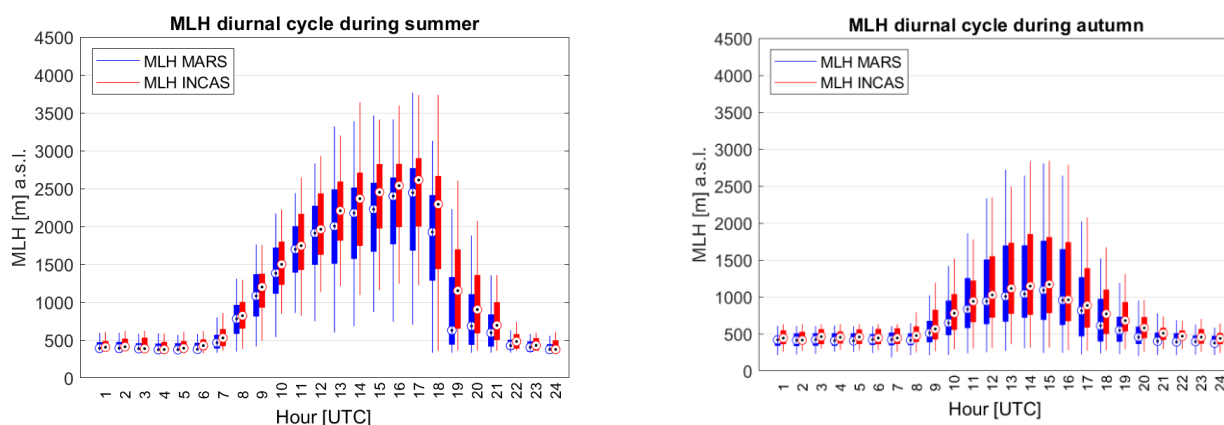


**Figure 5.2.** Diurnal cycle for MLH for the warm (left panel) and cold seasons (right panel) at reference site (MARS) and temporary site (INCAS).

### 5.3 Mobile measurements

Average near-surface particulate matter concentrations at different Bucharest districts are almost double in all areas in winter, comparing with summer period. While summer NO<sub>2</sub> average concentrations are higher than winter values, most likely due to increased traffic.

The district where CET Vest is located does not present significantly higher values for NO<sub>2</sub> during the summer, although higher values for particulate matter are pinpointed. Moreover, during the winter season, particulate matter concentrations observed in the CET Vest proximity are among the highest in Bucharest (Figure 5.1).

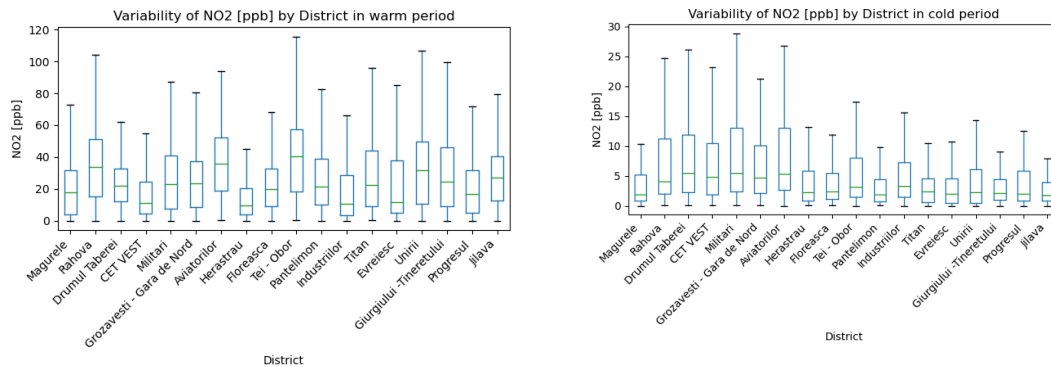


**Figure 5.3.** Average season near-surface NO<sub>2</sub> concentrations at different Bucharest districts as observed by mobile measurements (left panel: summer season; right panel: winter season).

The mobile data have been used to retrieve pollutant distribution maps with a horizontal resolution of 100 x 100 m using the strategy from RI URBANS mapping task (D27 (D4.6), Talianu et al., 2024). For this purpose, the ESCAPE Land Use Regression model, together with PyLUR tool and QGIS, was set up for Bucharest city. Furthermore, one-way two-level downscaling over the CET Vest Bucharest area had been performed to retrieve the NO<sub>2</sub> and PM<sub>10</sub> maps for both seasons at a horizontal resolution of 25 x 25 m.

The CET Vest does not contribute considerably to NO<sub>2</sub> concentrations during the warm season, when main source in the area is heavy traffic at the city's western exit. While during the winter season, the power plant produces larger concentrations and domestic heating becomes significant in the hotspot region (Figure 5.4). Particulate matter concentrations are more homogeneously distributed over the district, with higher values during winter but also higher gradients during summer. The high concentrations of PM<sub>10</sub> are associated to road dust, produced by construction and agricultural works, and transported by traffic. The power plant has no important roads in its vicinity and is not a source of large particles itself. Slightly higher concentrations of small particulate matter are measured in the power plant proximity the during the winter season.

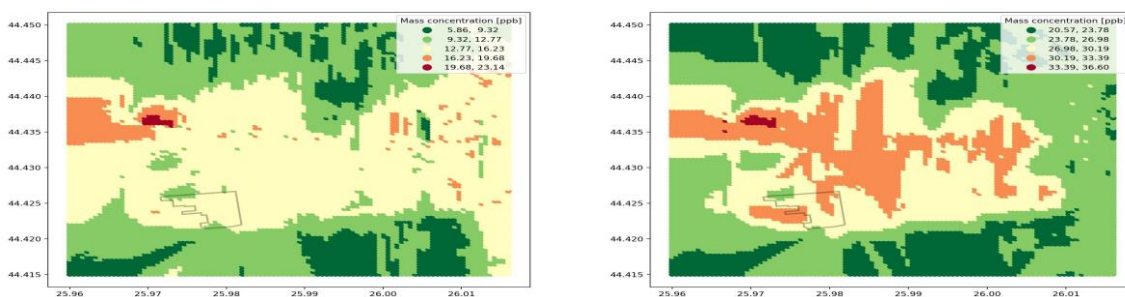


**Figure 5.4.** NO<sub>2</sub> distribution over West-Bucharest area: summer (left panels); winter (right panels); overlay with gradient mask. The location of the power plant is marked with black contour.

The most significant issue to be answered is whether the study region is more contaminated than the reference location, and whether the CET Vest power plant contributes to pollution in the near surface and upper troposphere. Based on the analysis conducted, our expectations that the CET Vest power plant could affect the air quality in the residential areas nearby is not confirmed. The only pollutant which can localize the power plant as a source is NO<sub>2</sub>, mostly during winter. Higher concentrations of particulate matter have been measured near the power plant, but the differences to other districts are not sufficiently large to allow a clear identification of the source. The fact that the differences to other districts are higher during the cold season may indicate that the power plant is a constant source of particles in the region (the power plant increases its operations during winter).

## 6. MILAN PILOT

The city of Milan, located in northern Italy (45°28'01"N 09°11'24"E), with a population of 3.22 million is one of the pilot cities in WP 4. The surrounding area of the metropolitan Milan is the rural Po Valley, a flat area hosting intense farming activities. The Alps in the North and the Apennine mountains in the South form a natural barrier to the area reducing the air ventilation and causing the atmospheric pollutants emitted from the urban as well as the rural areas to concentrate within the valley, which often experiences severe pollution episodes, mostly during wintertime. Milan hosts the city airport Milano Linate located about 7 km East of the city centre (45° 26' 34.79" N, 9° 16' 25.20" E) serving domestic, short distance and international flights within Europe. Our goal in 4.12 is to measure the total number concentration of particles and size, nitrogen oxides (NO<sub>x</sub>) concentrations, and black carbon concentration at Milano Linate airport, black carbon concentration within the urban area of Milan, with the final goal of evaluating pollutants concentrations at the pollution hot-spot sites -the airport and the urban area- compared with a background urban reference site.

### 6.1 Measurement strategy

We conducted three main activities during 2023-2024 to quantify the concentrations of the main pollutants from relevant sites in Milan and evaluate their impact for the city air quality. The first activity consisted of a 1-year-long measurement campaign at a background urban reference site in Milan where reactive gases (volatile organic compounds, nitrogen oxides, methane), carbon dioxide, black carbon concentration, particle chemical speciation, total particle concentration and size, were measured to serve as the reference site, for comparing the concentrations quantified at the pollution sites. Several ancillary measurements were carried out close to the site in parallel to the RI-URBANS activities through a collaboration involving the University of Helsinki, Milan, Frankfurt, and the Paul Scherrer Institute in order to characterize further pollution and atmospheric processes in the city. We will present some of these ancillary measurements in the section dedicated to the reference site.

The second activity consisted of an 8-months measurement campaign at the pollution hot-spot site of Milano Linate airport. In this campaign, we measured the total number concentration of particles and size, nitrogen oxides (NO<sub>x</sub>) concentrations, and black carbon concentration.

The third activity consisted in mapping the concentration of black carbon within the urban area of Milan with mobile measurements using micro-sensors installed on bikes of a bike-delivery company. This activity comprised four intensive campaigns of two weeks each, that took place over four seasons from autumn 2023 to summer 2024.

### 6.2 Background urban reference site

The CNR instruments were installed in a mobile laboratory parked at CNR Milan (45°28'47"N 9°13'54"E; 120 m a.s.l.) where the measurements were conducted. Ancillary measurements conducted by ARPA Lombardia, the Universities of Milan, Helsinki and Frankfurt and the Paul Scherrer Institute were conducted nearby, about 450 m

(Milano Pascal) and 800 m (University of Milan), distant from the CNR site. The CNR measurements started in January 2023 and ended in March 2024. The following parameters were measured:

- Chemical speciation of the non-refractory submicron particles (PM1) with an aerosol chemical speciation monitor (ACSM-ToF, Aerodyne, USA).
- Volatile organic compounds (VOCs) with a Vocus chemical ionization time of flight mass spectrometer (Vocus CI-ToF, ToFwerk, Switzerland).
- Methane (CH<sub>4</sub>) and carbon dioxide (CO<sub>2</sub>) with cavity ringdown spectroscopy (Picarro, USA).
- NO<sub>x</sub> with chemiluminescence (Thermo Scientific Model 42i-TL TRACE).
- BC with an aethelometer AE33 (Magee scientific, USA).

PM1 monthly mean mass concentrations and the chemical speciation during the cold and warm months are shown in Figure 6.1. Larger concentrations were measured during the cold months, when particles were composed of organics (42%), followed by nitrates (36%), ammonium (13%), sulphate (8%) and less than 1% of chlorine. In contrast, during the warm months, PM1 concentrations were smaller but the organic fraction was dominant, representing 67% of the chemical components.

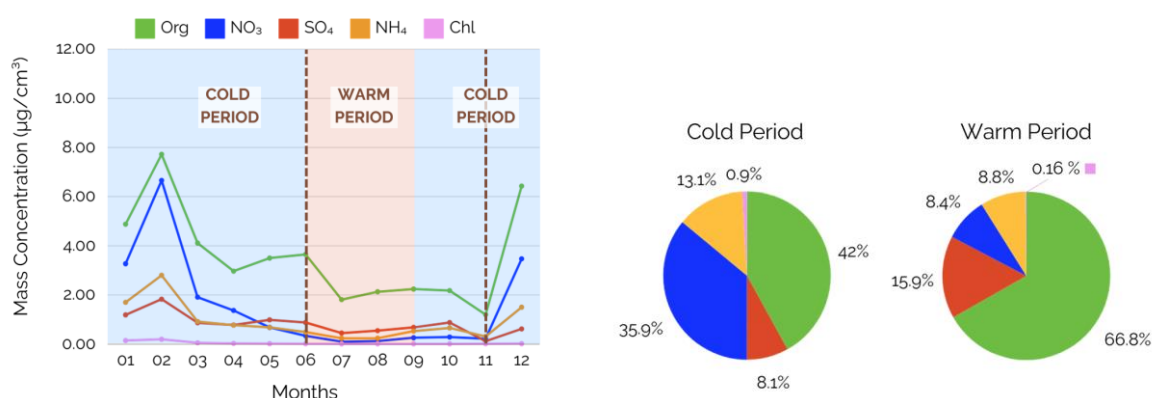


**Figure 6.1.** Monthly mean mass concentrations of the non-refractory submicron aerosol species identified with an ACSM-ToF. Months were classified according to the air temperature monitored at the site and the chemical speciation of the respective time periods is reported in the pies.

VOC were measured in order to better elucidate the organic precursors involved in the formation of secondary organic aerosols (SOA) measured at the site. Figure 6.2 illustrates the diel patterns of four different VOC with a remarked different origin and physical-chemical properties. Their different origin, and chemical nature is reflected in the different diel patterns and seasonality, as well as in their normalized measured concentrations. Benzene (Figure 6.2C) and toluene (Figure 6.2D), emitted from fossil fuel combustion, have normalized mixing ratios with two peaks during the day, a morning peak and an evening peak, associated with traffic emissions during the rush hours. The occurrence of those two peaks is slightly shifted in time in winter and summer, reflecting human activities in standard and daylight-saving times. While benzene normalized mixing ratios are nearly the same in the two inspected seasons, toluene normalized mixing ratios are almost double during winter compared with summer. Different diel patterns are found for acetone (Figure 6.2A), a secondary VOC, and isoprene (Figure 6.2B), primarily emitted from plants. Acetone shows a morning peak that may reflect the start of photochemical activities, or any other emission, larger in winter than in summer. Isoprene, in contrast, is more emitted during summer than in winter, with a sustained large mixing ratio during the day in summer, reflecting plants photosynthetic activity.

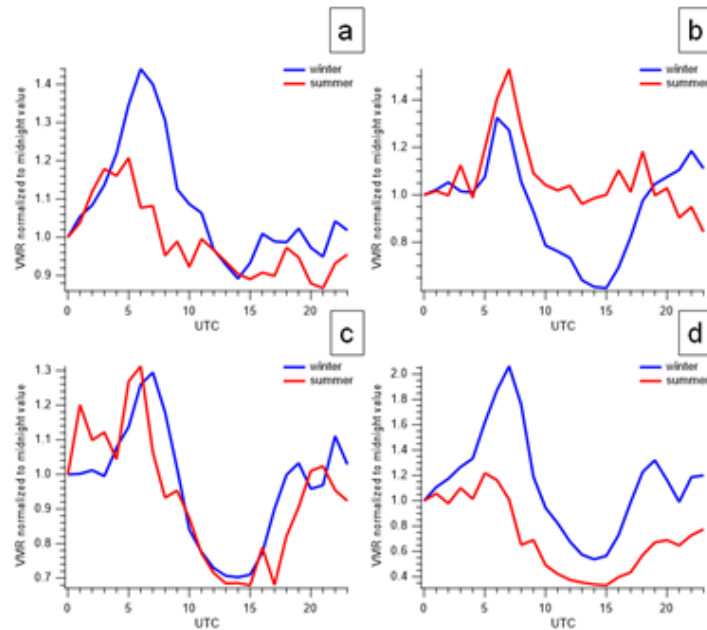


**Figure 6.2.** Normalized to midnight values median mixing ratios of acetone (a), isoprene (b), benzene (c) and toluene (d) measured during summer and during winter.

CO<sub>2</sub>, CH<sub>4</sub>, and NO<sub>x</sub> concentrations measured from August to March are reported in Figure 6.3. These three parameters show larger concentrations during the months of December 2023 to February 2024 compared with the summer months.

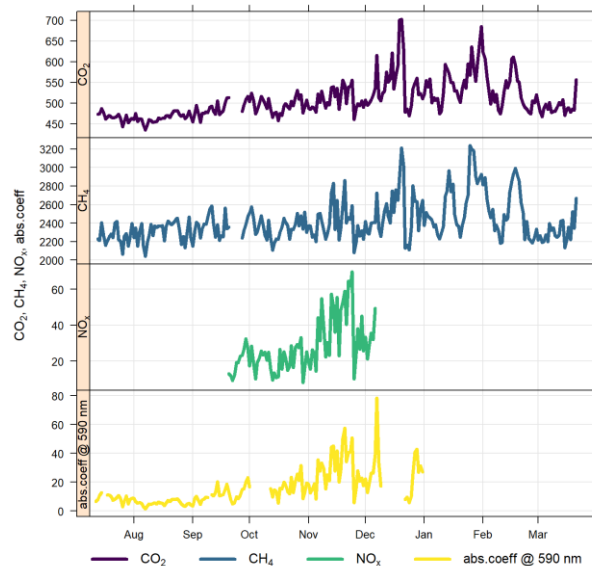


**Figure 6.3.** Concentrations of CO<sub>2</sub>, CH<sub>4</sub>, NO<sub>x</sub> and absorption coefficient at 590 nm nt at 590 nm measured from August 2023 to March 2024.

As ancillary measurements, ARPA Lombardia made available all the data for the parameters measured at the Pascal site, which are:

- Daily concentrations and chemical composition of PM<sub>10</sub> and PM<sub>2.5</sub> using a dual-head sampler (FAI DC) and subsequent chemical-physical analyses (ED-XRF, IC, Sunset).
- Hourly equivalent BC (eBC) concentrations with an aethalometer AE33 (Magee Scientific) and a MAAP 5012 (Thermo Scientific).
- Hourly total carbon measurements with a TCA08 (Magee Scientific).
- Hourly Aerosol scattering and backscattering measurements at 3 λ with a nephelometer (Ecotech Aurora 3000).
- Hourly O<sub>3</sub> concentrations (TEI 49i).
- Hourly NO<sub>x</sub> concentrations (API 201);
- Hourly VOC C<sub>6</sub>–C<sub>12</sub> concentrations (GC955 Syntech).
- Hourly SO<sub>2</sub> concentrations (TEI 43i).
- Hourly CH<sub>4</sub>-CO<sub>2</sub>-N<sub>2</sub>O concentrations (Picarro 2509).
- Hourly Ammonia (NH<sub>3</sub>) concentrations (Picarro 2509 and Chemiluminescence API 201).

Near the site, meteorological parameters are collected as well. The chemical speciation of PM<sub>10</sub> during 2023 is reported in Figure 6.4.

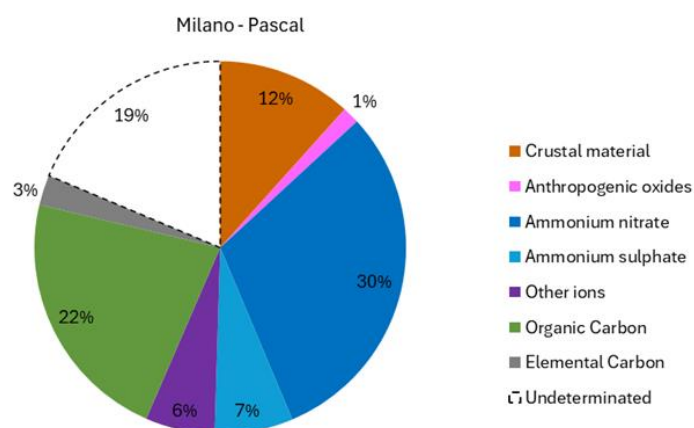


**Figure 6.4.** PM<sub>10</sub> composition during 2023 in MI-Pascal.

Atmospheric aerosols have been sampled at Milan-Pascal site since March 2023 with 24-hour time-resolution. Additionally, four intensive campaigns have been conducted to increase the sampling time resolution to 6 hours.

Two high volume samplers have been deployed in order to collect PM<sub>10</sub> and PM<sub>2.5</sub> fractions on quartz fibre filters (PALL, Ø=150 mm). The Goethe-University Frankfurt (Frankfurt am Main, Germany) plans to perform chemical analysis on a subset of the PM<sub>2.5</sub> fraction filters to achieve the molecular characterization of the organic compounds by means of high-resolution and high-accuracy mass spectrometry (HRMS, Orbitrap MS) after compounds separation with ultra-high-performance liquid chromatography (UHPLC). The eluted compounds will be ionized using a soft ionization technique, including heated electrospray (HESI) or atmospheric pressure chemical ionization (APCI), both in positive and negative mode. This approach aims to provide a comprehensive investigation of the ionizable organic phase forming PM<sub>2.5</sub> particles. Non-targeted analysis will be used to take into account the

overall complexity of the organic aerosol system, supported by accurate formula attribution (<2 ppm). In addition, specific markers of both anthropogenic and biogenic sources will be targeted for confirmation.

To ensure consistent performance of the UHPLC-HRMS analysis method, chemical analyses will be carried out after the collection of all filters, scheduled for completion at the end of July 2025.

Among the ancillary activities nearby the CNR site, the University of Helsinki measured particle number size distribution of particles with diameter between 1.2 to 480 nm between April 2023 and April 2024, with the goal of characterizing ultrafine particle number concentrations and studying the process of New Particle Formation (NPF).

The measurements were performed in the Chemistry and Physics Departments of the University of Milano with a set of three instruments: a nano-Condensation Nucleus Counter (nCNC - 1.2 and 3 nm), a Nuclear Cluster and Air Ion Spectrometer (NAIS - 2.5 and 40 nm) and a Scanning Mobility Particle Sizer (SMPS - 10 and 480 nm).

The analysis of the data points out the seasonality of size distribution (Figure 6.5). In winter, larger particles (>100 nm) increase due to reduced boundary layer height and heating emissions, with traffic-related peaks at rush hours. In spring and summer, traffic-related peaks diminish due to enhanced atmospheric mixing, while sub-10 nm particles surge midday, driven by photochemical reactions under higher solar radiation. Summer sees the highest sub-10 nm levels but the lowest >100 nm particle concentrations. In autumn, cooling temperatures and reduced dispersion revive traffic-related peaks, with overall concentrations resembling spring.

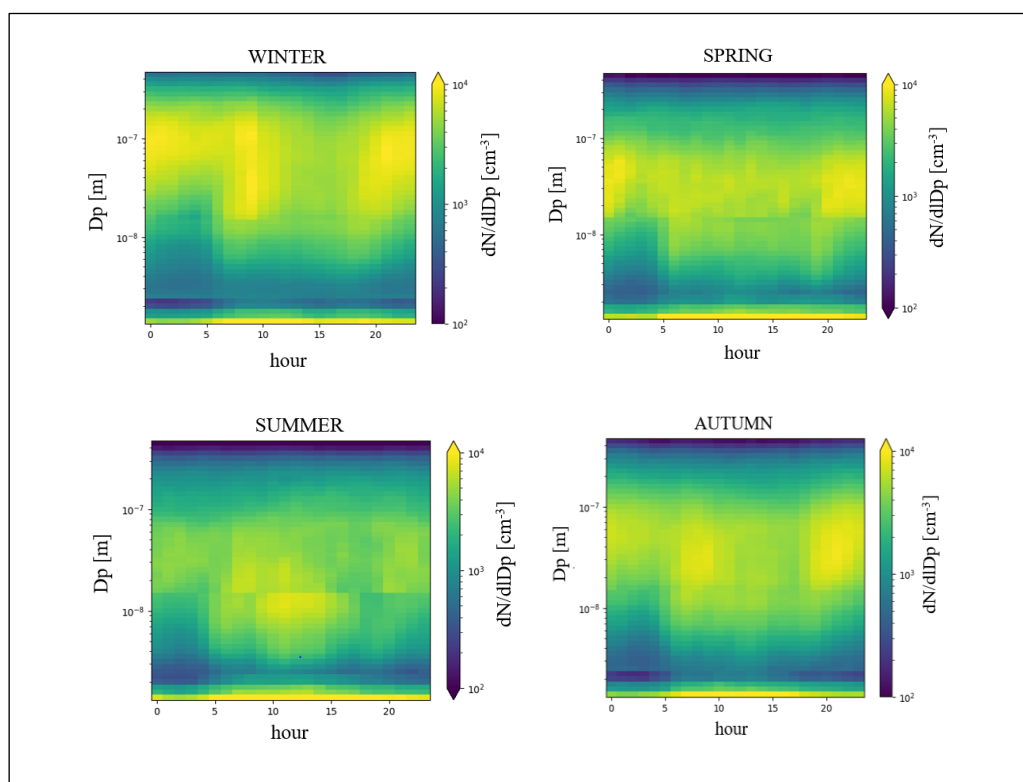


**Figure 6.5.** Surface plot of particle number size distribution in winter, spring, summer and autumn.

The study of NPF, conducted using the nano-ranking method, confirms that NPF events are most frequent and intense during summer, with reduced activity during winter. Analysis of NPF intensity in relation to pollutant concentrations and dispersion variables reveals that new particle formation is promoted by a “cleaner” atmosphere, characterized by lower levels of condensation sink, PM<sub>10</sub>, PM<sub>2.5</sub>, NO<sub>x</sub>, SO<sub>2</sub>, and BC, and enhanced atmospheric mixing, indicated by a higher ventilation index.

Strong NPF events are particularly associated with north-westerly winds, especially under foehn conditions, which significantly enhance particle formation. Day-by-day analysis shows that these winds create more favourable conditions for intense NPF. To further investigate the influence of air mass characteristics on NPF processes, a Lagrangian particle dispersion model was employed alongside high-resolution meteorological models.

The combined modelling and particle size distribution data confirm that north-westerly airflow is the most favourable for NPF. The modelling analysis also shows that, cleaner air masses, with limited exposure to anthropogenic pollution and reduced time spent in the Po Valley region, further enhance the conditions for NPF (Figure 6.6). A paper about NPF dynamic in Milano is under preparation.

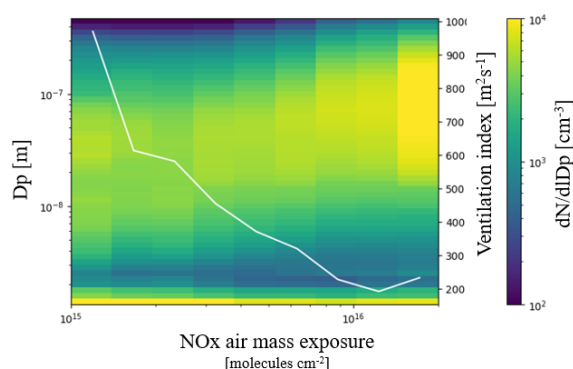


**Figure 6.6.** The relationship between air mass exposure to NO<sub>x</sub> sources, the ventilation index, and particle diameter demonstrates that lower air mass exposure to NO<sub>x</sub> sources and higher ventilation index values correspond to smaller particle diameters, supporting the hypothesis that these conditions enhance the strength of new particle formation (NPF).

Another study that was performed (by UNIMI, ARPA and PSI) in parallel to RI-URBANS activities was the inter-comparison between on-line (XACT by PSI) and benchtop (ARPA laboratory equipment) EDXRF measurements. Results show a good agreement and assess the reliability of on-line XRF spectrometers in monitoring networks. A paper is under preparation.

Lastly, data from a 7-l Aethalometer and a 3-l Nephelometer (both available at the ARPA MI-Pascal monitoring station) were collected for 1 year and analysed (by UNIMI) as for the absorption and scattering coefficients, respectively. First scattering data for the Milan urban area were retrieved. Optical source apportionment and aerosol typing based on optical intensive variables was performed highlighting the potential application of such approach for near real-time identification of specific aerosol types. A paper is under preparation.

### 6.3 Milano Linate Hot-Spot site

Measurements at Milano Linate airport were conducted from a mobile laboratory parked in the airport parking, where the instruments were installed to measure the following parameters:

- Aerosol size distribution 10nm-800nm using a scanning mobility particle sizer (SMPS, Tropos, Germany).
- Aerosol size distribution 300 nm-10 µm using an aerosol particle sizer and an optical particle counter (APS, TSI, USA and OPC, Grimm, Germany).
- eBC concentration with an aethalometer AE33 (Magee scientific, USA).
- Aerosol scattering and backscattering coefficients at 3 λ with a nephelometer (Ecotech Aurora 3000 Integrating Nephelometer, Acoem, Sweden).
- Meteorological parameters

Our study focused on understanding the variability of eBC concentration measured at the site with the time of the day and season with respect to the atmospheric dynamics, in particular to the mixed aerosol layer height obtained from remote sensing techniques, here representing a proxy for the planetary boundary layer height. eBC concentration was largest during wintertime, and decreased during spring and summer. As expectable, the mixed aerosol layer height was largest in summer, and decreased during winter and spring. The opposite behaviour between black carbon concentration and the mixed aerosol layer height is visible in the time series across different seasons (Figure 6.7) and in the diel profiles of two months of campaign (Figure 6.8). Figure 6.8 shows also the opposite behaviour between the mixed aerosol layer and the total particle number concentration.

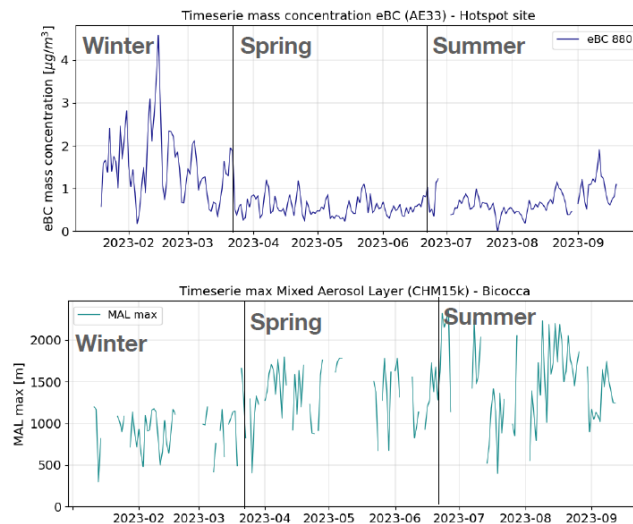


**Figure 6.7.** Equivalent black carbon mass concentration and mixed aerosol layer maximum height across three seasons in Milan.

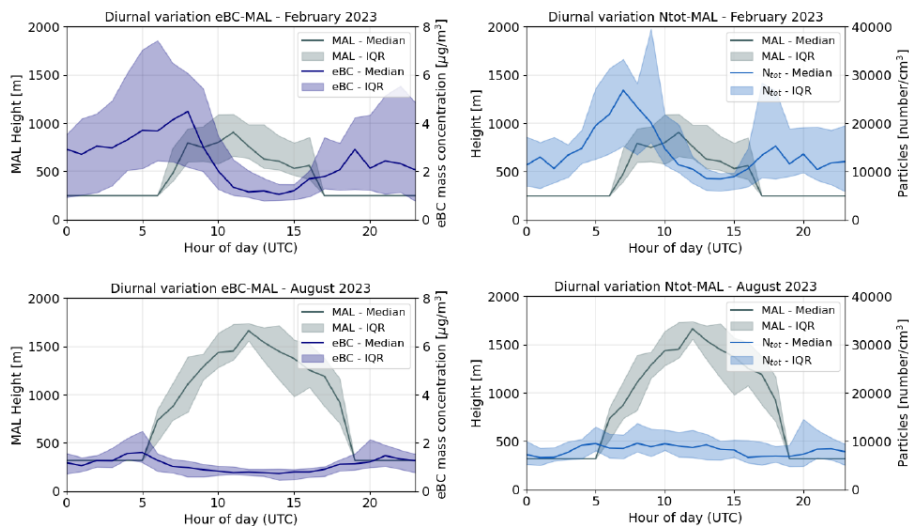


**Figure 6.8.** Diel profiles of equivalent black carbon mass concentration and total particle number concentration measured during February and during August 2023 at Milano Linate. Mixed aerosol layer height retrieved from measurements using a ceilometer (CHM15k) installed at the University of Milano Bicocca (urban background site). Lines represent median values while shaded areas represent the interquartile range.

#### 6.4 Urban mapping with mobile measurements

BC concentrations were monitored across the streets of Milan downtown using micro-Aethalometers (microAeth®, models AE51 and MA200, AethLabs, San Francisco, CA, USA) mounted on the bikes of the local courier delivery company: Urban Bike Messengers (UBM). The micro-Aethalometers AE51 and MA200 are portable filter-based absorption photometers that follow the same operational principle as the stationary version AE33, except that AE51 reports BC only at 880 nm and does not apply an online correction for loading.

The measurements were collected following an opportunistic approach, for which the sampling route was determined by the delivery routes, tracked by GPS sensors. During each seasonal 2-weeks campaign, an area of nearly 25 km<sup>2</sup> was covered by the couriers from Monday to Friday between 9:00 and 18:00 CEST (with a break at noon) measuring eBC at 30, 10 and 1-sec time resolutions, and with average flow rates of 150 ml min<sup>-1</sup>. When available, two samplers were paired on each bike, one of each model of aethalometer, to assess the repeatability of the measurements. During the campaigns frequent controls of flow rate, zero and noise levels, as well as overnight comparisons with the urban background reference were performed to assure the quality of the data collected.

The data obtained from the portable samples during the measurements campaigns was later post processed and corrected for flow and loading effect. The different comparisons with the reference instruments showed a maximum average difference with respect to the reference of 10%, with R<sup>2</sup>>0.7. Moreover, the geo-position records were taken at an average 30-second time resolution due to technical limitations of the GPS sensors, for which the position of the samplers between to records of positional data were interpolated to match the time resolution of the eBC monitors. Finally, the eBC concentrations can be paired with their corresponding geolocation, and projected into city maps that can allow the visual identification of pollution hotspots, which will be presented in the following section.

The preliminary results presented in this report include only the periods in which the samplers were deployed away from the company's headquarters, across the sampling delivery routes. Figure 6.9 displays the daily variability of BC concentrations measured by the portable samplers (Mobile) and by the reference instruments at the urban background stations (Mi-CNR and Mi-Pascal, during similar periods), in two very contrasting seasons. It can be observed that the difference between the near-road concentrations and the urban background concentrations changes across the seasons and throughout the day, being maximum during the early morning hours in winter. The reasons for this could be the poor dilution happening in the mixing layer at low temperatures, as well as the presence of additional sources such as residential heating.

From a spatial perspective, in Figure 6.10 are displayed the near-road BC concentrations normalized by the hourly-seasonal average, to remove temporal variability. On the left panel are plotted in blue the eBC concentrations that were below the median (i.e.: norm eBC <1), on the right panel are the concentrations above the median (i.e. nom BC >1). The normalized median eBC concentrations > 1 in Figure 6.10 clearly outline the beltway and radial streets of the city of Milan in which typically the number of vehicles but also traffic congestion is expected to be the largest. In contrast, the normalized concentrations <1 cover the areas in between the arterial streets.

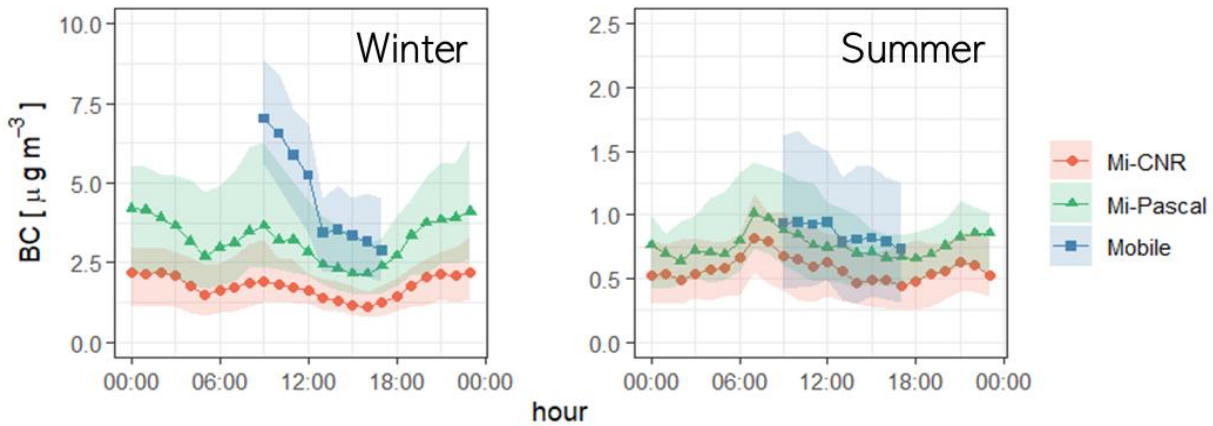


**Figure 6.9.** Diurnal variability of hourly median eBC concentrations measured near-road during the winter and summer campaigns using the portable absorption photometers AE51 and MA200 (blue squares), compared to the eBC concentrations measured by the stationary reference absorption photometers AE33 at the urban background stations Milano-CNR (red) and Milano-Pascal (green) during comparable periods. The coloured shaded area around the median represents the corresponding interquartile ranges.

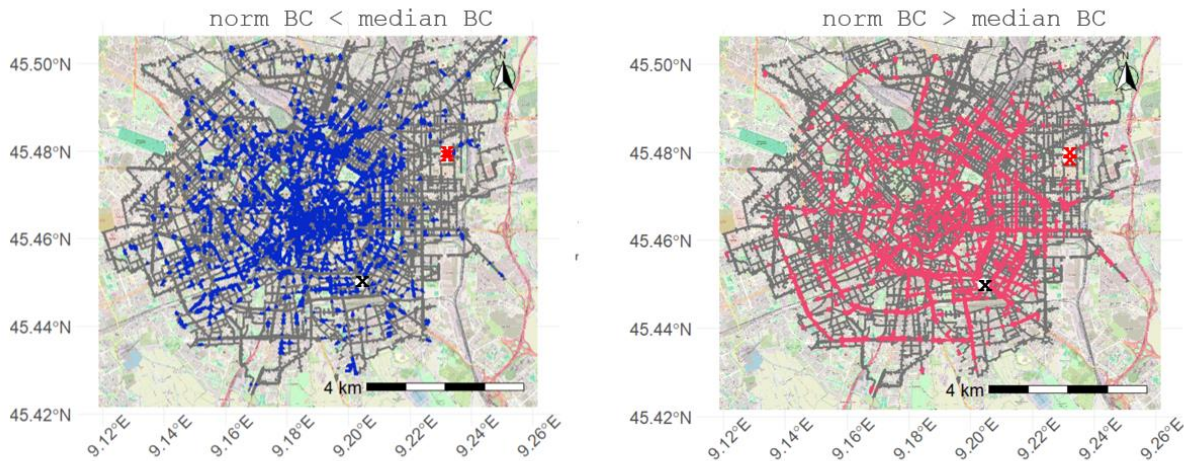


**Figure 6.10.** Median normalized eBC concentrations measured during the four seasonal campaigns separated by their ratio with respect to the hourly-seasonal median near-road concentrations. In blue on the left panel are displayed the concentrations that were found below the near-road median concentrations. On the right panel are plotted the normalized concentrations higher than the near-road median. The red 'X's mark the position of the two urban background stations.

### 6.5 Comparison between hot spot-sites and reference site

We compared the results obtained from the hot-spot sites (the airport and the urban area) with those obtained from the reference site for those measurements common to the three sites, particularly black carbon mass concentration and common to two sites, such as total particle number concentration.

eBC concentration was largest in winter, followed by autumn, spring and summer, anywhere (Figure 6.11). The concentrations reported from the two reference sites which are close to each other are in good agreement. eBC concentrations measured at Linate airport and in the urban area appear to be overall larger than the concentrations measured at the urban background reference sites, during any season, with more pronounced differences between the urban area and the reference sites during wintertime.

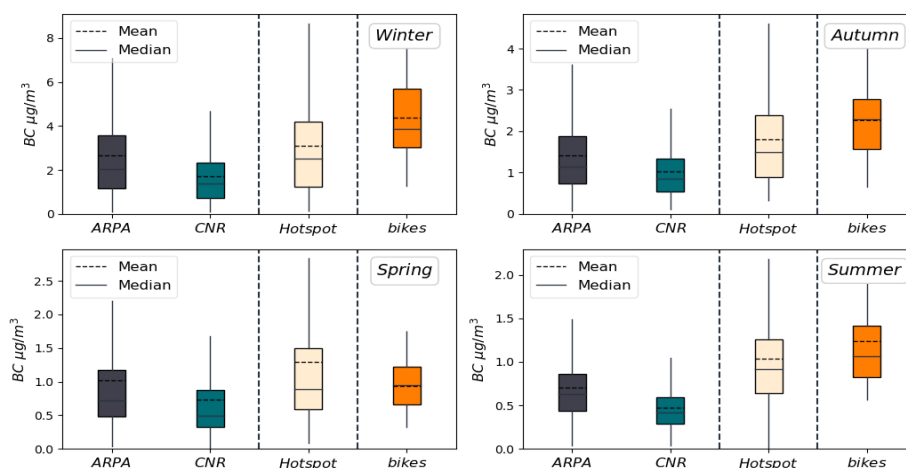


**Figure 6.11.** Seasonality of eBC concentration measured in the urban area of Milan (bikes), at the airport (hotspot) and at two urban background sites (CNR, the reference background site and the nearby ARPA Mi-Pascal).

In contrast with what was observed for black carbon, the total particle number concentration was substantially larger at Linate airport compared with the reference urban background site (Figure 6.12).

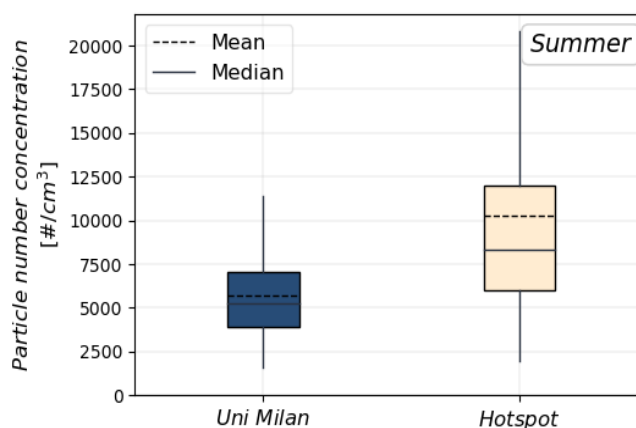


**Figure 6.12.** Particle number concentration in the size range 10-800 nm measured with a scanning mobility particle sizer (SMPS, TSI, USA) during summertime in Milan. The hot-spot pollution site is compared with the background site (“Uni Milan”). The box plot shows mean, median and 25-75 percentiles values.

## 7. POTENTIAL FOR SUSTAINABILITY AND UPSCALING IN CITIES

The new Ambient Air Quality Directive (EU) 2024/2881 is requiring that the highest pollution hotspots should be identified and air quality measurements carried out there, with a ratio urban background/hotspot ratio not higher than 2. The methods used here are valid for this identification, not only for new pollutants but also for criteria pollutants. In this sense the mapping of pollutants at urban scale is a very powerful tool for implementing this new directive.

The pilot studies performed for characterisation of pollution hot-spots in the framework of the RI-URBANS project in the cities of Rotterdam, Bucharest and Milano have shown that advanced observations have added value to the understanding of exposure to air pollution in general and UFP in particular.

The pilot studies using remote sensing instrumentation have shown that valuable data can routinely be acquired from strategically located ceilometers and Doppler wind lidars in order to assess the atmospheric dynamics that drive the dispersion of air pollution. The technical readiness of these instruments is operational and should be ready to provide data for model validation in any urban environment. In a next step, coupling of the data to models and assimilation should provide a further step in forecasting of air pollution episodes. However, this still remains a challenge.

The remote sensing of NO<sub>2</sub> concentration maps provides insights that can be very useful for understanding specific cases, since the instrumentation is not fully mature and only campaign-based observations are feasible. Nevertheless, this could be interesting to apply in other cities, so as to get a better understanding of, for instance, the changes in terrain on the dispersion of air pollution from the hot-spots. Also, validation of satellite observations that are sparser and of coarser resolutions is useful to apply in various cities.

Mobile observations provide great insight in characterisation of pollution hot-spots. Once instrumented vehicles are available, they can be deployed in all kinds of cities. However, how often such campaigns should and could be conducted and under what kind of circumstances should be carefully considered, as the collection is laborious and therefore costly.

The bicycle measurement approach during RITA-2022 demonstrates that mobile measurement campaigns combined with citizen participation are an effective method to obtain detailed urban air quality data. The approach offers the potential to validate urban air quality models: In the future, the mobile bicycle measurements collected could be used to validate urban air quality models such as the RETINA urban air quality system for the Rotterdam area. The conditions for a wider application of citizen operated bicycle measurements of NO<sub>2</sub> and eBC are seen as follows: *Availability of measurement equipment:* Accurate and portable equipment must be available to measure NO<sub>2</sub> (and/or other components rapidly varying in urban air pollution such as BC). In addition to high measurement accuracy, this equipment must be able to detect both background NO<sub>2</sub> concentrations down to at least 1 ppbv (detection limit) and high concentrations within plumes (e.g. from nearby traffic emissions). Furthermore, rapid fluctuations in concentration must be detectable from a moving platform, which requires a sensor response time of approximately 1 Hz. Ultimately, the sensor should withstand challenging atmospheric conditions like fluctuating ambient temperature, humidity, and rainfall, while also being adequately selective for NO<sub>2</sub>. To our knowledge, the KNMI NO<sub>2</sub>-sonde is currently the only instrument that meets these specific specifications. Unfortunately, this instrument is not yet commercially available, which presently limits its applicability to occasional atmospheric measurement campaigns. *Logistical support:* A clearly defined measurement route and support from local organisations or universities are essential. *Citizen involvement:* Active citizen participation is crucial, requiring adequate information/communication and motivation to participate in the experiment. *Repeatability of the route:*

Continuously cycling the same route helps to increase data representativity and provides more consistent insights compared to changing the route with every cycle.

Finally, this the hot-spot pilot shows that a combined use of various techniques, in-situ and remote sensing, will gain the most complete dataset to address the pollution studies for a particular city, especially in cases of complex (orographic) terrain, or large/mega cities with very complex building structures.

## 8. REFERENCES

- Baxter, L.K., Dionisio, K.L., Burke, J., Sarnat, S.E., Sarnat, J.A., Hodas, N., Rich, D.Q., Turpin, B.J., Jones, R.R., Mannshardt, E., 2013. Exposure prediction approaches used in air pollution epidemiology studies: key findings and future recommendations. *J. Expo. Sci. Environ. Epidemiol.* 23, 654-659. <http://dx.doi.org/10.1038/jes.2013.62>
- Kerckhoffs J, Hoek G, Messier KP, Brunekreef B, Meliefste K, Klompmaaker JO, Vermeulen R. Comparison of Ultrafine Particle and Black Carbon Concentration Predictions from a Mobile and Short-Term Stationary Land-Use Regression Model. *Environ Sci Technol.* [2016;50\(23\):12894-12902](https://doi.org/10.1021/acs.est.5b02894).
- Kerckhoffs J, Hoek G, Vlaanderen J, van Nunen E, Messier K, Brunekreef B, Gulliver J, Vermeulen R. Robustness of intra urban land-use regression models for ultrafine particles and black carbon based on mobile monitoring. *Environ Res.* [2017;159:500-508](https://doi.org/10.1016/j.envres.2017.05.008).
- Kumar, P., Morawska, L., Martani, C., Biskos, G., Neophytou, M., Di Sabatino, S., Bell, M., Norford, L., Britter, R., March 2015. The rise of low-cost sensing for managing air pollution in cities. *Environ. Int.* 75, 199-205, [10.1016/j.envint.2014.11.019](https://doi.org/10.1016/j.envint.2014.11.019)
- Shen Y, de Hoogh K, Schmitz O, Clinton N, Tuxen-Bettman K, Brandt J, Christensen JH, Frohn LM, Geels C, Karssenberg D, Vermeulen R, Hoek G. Europe-wide air pollution modeling from 2000 to 2019 using geographically weighted regression. *Environ Int.* 2022 Oct;168:107485. doi: [10.1016/j.envint.2022.107485](https://doi.org/10.1016/j.envint.2022.107485)
- Talianu, C., Vasilescu, J., Nicolae, D., Ilie, A., Dandocsi, A., Nemuc, A., and Belegante, L.: High-resolution air quality maps for Bucharest using Mixed-Effects Modeling Framework, EGUsphere [preprint], <https://egusphere.copernicus.org/preprints/2024/egusphere-2024-2930/>
- Kotthaus, S., Bravo-Aranda, J. A., Collaud Coen, M., Guerrero-Rascado, J. L., Costa, M. J., Cimini, D., O'Connor, E. J., Hervo, M., Alados-Arboledas, L., Jiménez-Portaz, M., Mona, L., Ruffieux, D., Illingworth, A., and Haeffelin, M.: Atmospheric boundary layer height from ground-based remote sensing: a review of capabilities and limitations, *Atmos. Meas. Tech.*, 16, 433–479, <https://doi.org/10.5194/amt-16-433-2023>, 2023
- Fry, Juliane L. and Ooms, Pascale and Krol, Maarten and Kerckhoffs, Jules and Vermeulen, Roel and Wesseling, Joost and van den Elshout, Sef, *Effect of street trees on local air pollutant concentrations (NO2, BC, UFP, PM2.5) in Rotterdam, the Netherlands, Environmental Science: Atmospheres, 2025*, <https://doi.org/10.1039/D4EA00157E>
- Mijling, B.: High-resolution mapping of urban air quality with heterogeneous observations: a new methodology and its application to Amsterdam, *Atmos. Meas. Tech.*, 13, 4601–4617, <https://amt.copernicus.org/articles/13/4601/2020/>.
- Sluis, W. W., Allaart, M. A. F., Piters, A. J. M. and Gast, L. F. L.: *The development of a nitrogen dioxide sonde*. *Atmos. Meas. Tech.*, 3, 1753–1762 <https://amt.copernicus.org/articles/3/1753/2010/>.